



1 **Coupling of numerical groundwater-ocean models to improve**
2 **understanding of the coastal zone**

3 Jiangyue Jin^{1,2,3}, Manuel Espino^{1,3}, Daniel Fernández^{1,2}, Albert Folch^{1,2}

4 ¹Department of Civil and Environmental Engineering (DECA), Universitat Politècnica de Catalunya (UPC), Barcelona 08034,
5 Spain

6 ²Associated Unit: Hydrogeology Group (UPC-CSIC), Spain

7 ³Laboratori d'Enginyeria Marítima (LIM)

8 *Correspondence to:* Jiangyue Jin (Jiangyue.Jin@upc.edu)

9 **Abstract.** Coastal zones are increasingly acknowledged as dynamic yet fragile components of global ecosystems amidst
10 escalating anthropogenic activities and complex land-ocean interactions. Understanding the interactions between groundwater
11 and the ocean is crucial for managing submarine groundwater discharge (SGD) and seawater intrusion (SWI), vital for coastal
12 ecosystem preservation and water resource management. This research proposes an integrated modeling approach that couple
13 groundwater flow and physical oceanographic models to accurately simulate coastal-ocean groundwater interactions.

14 In this work, a TELEMAC-3D based three-dimensional hydrodynamic model was initially developed to capture marine
15 conditions with variable salinity and temperature. A MODFLOW6 groundwater model was subsequently constructed. The models
16 were efficiently coupled using Flopy and Telapy, enabling precise co-simulation of hydrodynamic and groundwater systems.
17 Validation of the coupled model against empirical data confirmed its high fidelity, with errors within acceptable ranges.

18 This coupled model employs dynamic boundary conditions, overcoming the limitations of traditional coastal groundwater
19 models that assume constant salinity. This enhancement significantly improves the accuracy and practicality of simulating SGD
20 processes in the coastal ocean. The bidirectional feedback mechanism within the coupled model strengthens the analysis of
21 interactions between the ocean and groundwater systems. It accounts for variations in the seawater boundary under tidal influence
22 and the reciprocal impact of groundwater dynamics on the hydrodynamic conditions of nearshore waters. This holistic
23 enhancement bolsters the model's hydrological simulation capabilities, providing a more comprehensive depiction of the intricate
24 water-salt exchange mechanisms in coastal systems.

25

26 **Keywords** Coastal zone modeling, SGD, SWI, Coupled model, Telemac, Telapy, Modflow6, Flopy, Groundwater-ocean
27 interaction



1 **1 Introduction**

2 The coastal zone, a critical ecological interface where land and sea intersect, carries a unique ecological environment and
3 important functions in the global ecosystem (Turner et al., 1996). Its dynamic balance is increasingly affected by human activities
4 and the intensification of land-sea interactions, making it one of the most vibrant and sensitive parts of the Earth (Ramesh et al.,
5 2015). Faced with the dual pressures of environmental change and human activities, it is particularly crucial to deeply understand
6 the interactions among various parts of the Earth's water cycle system, especially in the coastal zone where the ocean and land
7 meet. Among them, the interaction between the ocean and the terrestrial groundwater system, especially seawater intrusion (SWI)
8 (Kim et al., 2015) and submarine groundwater discharge (SGD) (Lin et al., 2024), has profound impacts on the hydrological cycle,
9 water resource quality (Santos et al., 2021), ecosystem health, and global material cycle in the coastal zone (Cao et al., 2021).

10 As the phenomenon of seawater intrusion caused by over-extraction of groundwater intensifies, marine ecosystems are
11 facing serious threats, manifested as the decline of ecosystems such as bays, estuaries, and coastal wetlands. At the same time,
12 groundwater pollution (Perumal et al., 2024) is an urgent problem to be solved, which not only affects water quality, but may
13 also introduce pollutants into the ocean through the SGD pathway, further deteriorating seawater quality and causing long-term
14 damage to the ecosystem (Moore & Joye, 2021). In addition, eutrophication of water bodies (Dong et al., 2024) and hypoxic
15 events (Wang et al., 2022) have also become severe challenges facing the current coastal environment, exacerbating the pressure
16 on aquatic ecosystems.

17 In the face of these challenges, researchers are concurrently focusing on the interactions between groundwater
18 systems (Martínez-Pérez et al., 2022) and marine ecosystems (Ramatlaping et al., 2021) to deeply analyze the intrinsic connection
19 between groundwater dynamic changes and marine ecological problems (Fang et al., 2021a). Developing models that accurately
20 represent the dynamic interactions between groundwater and ocean systems is essential for a deeper understanding and better
21 management of these interconnected environments.

22 Although traditional coastal groundwater studies have considered boundary conditions such as tidal changes and sea level
23 variations when assessing SWI (Yu et al., 2019). Most research still treats the ocean as a static boundary, overlooking the dynamic
24 impact of ocean dynamics on groundwater migration rules (Nguyen et al., 2020). Similarly, oceanographers highly value factors
25 such as waves, tides, and currents when exploring the interface processes between surface water and the ocean. However, they
26 often overlook the potential contribution of groundwater as an important terrestrial water source to the chemical composition,
27 thermodynamic state, and ecosystem functions of the ocean. When constructing ocean models, the influence of groundwater is
28 typically not considered (Arévalo-Martínez et al., 2023). Therefore, developing comprehensive models that can accurately depict
29 these complex dynamic processes is crucial for effective management and quantification of internal processes both in coastal
30 waters and in coastal aquifers.

31 Recent interdisciplinary research has clearly pointed out that relying solely on independent surface water models or
32 groundwater models is insufficient to fully reveal the essential characteristics of complex hydrological processes in coastal
33 zones (Arévalo-Martínez et al., 2023). Especially the bidirectional coupling between groundwater and the ocean (Dassargues et
34 al., 1996), including the impact of groundwater on the marine environment and the feedback effect of ocean dynamics on the
35 dynamics of the groundwater system, is not fully expressed in traditional separate models (Lewandowski et al., 2020). Therefore,
36 the development of coupled models that can simultaneously simulate and integrate the interactions between groundwater and the
37 ocean has become an urgent task in academic research.

38 In the practice of constructing ocean-groundwater coupled models, researchers have encountered a series of significant
39 technical challenges (Haque et al., 2021). First, how to solve the problem of system scale and dynamic differences is a key
40 difficulty in integration (Carabin & Dassargues, 1999). When building ocean models, groundwater is usually not considered, rapid
41 hydrological phenomena such as tides need to be simulated with high accuracy, which usually requires a fine spatial grid
42 resolution; in contrast, groundwater models focus on groundwater flow movement at larger scales, paying attention to relatively
43 slow hydrological cycles, resulting in prominent problems of mismatched grid size and time scale. At the same time, achieving
44 synchronous operation of coupled models on different time frames is also a daunting task (Yang et al., 2013a). Ocean models
45 often track rapidly changing ocean dynamics on an hourly scale, while the calculation period of groundwater models may be in



1 days or weeks. To realistically simulate the interaction between the two in the actual environment, it is urgent to find effective
2 means to coordinate the simulation consistency of the two models at different time and space scales, to overcome the
3 aforementioned integration problems, and to ensure that the coupled models can accurately describe complex hydrological
4 processes, salinity distribution, pollutant transport, and nutrient cycling in coastal areas(Liu et al., 2023).

5 At the interface between groundwater and seawater, due to the physical property differences of the media (seawater flows
6 in an open marine environment, while groundwater flows in porous media) and the momentum differences between seawater and
7 groundwater, the speed of seawater entering groundwater may significantly decrease, while the impact of groundwater entering
8 seawater on the speed of seawater may be relatively small(Slomp & Van Cappellen, 2004). Therefore, when simulating the
9 interaction process between groundwater and seawater, we may not need to consider the speed changes at the interface in detail.
10 However, this does not mean that speed has no impact on the interaction process between groundwater and seawater. For instance,
11 changes in speed may affect the transport and diffusion of substances, thereby affecting the material exchange between
12 groundwater and seawater(Michael et al., 2005).

13 The aim of this study is to propose a coupling method between an ocean hydrodynamic model and a groundwater flow
14 model while quantitatively assessing the interaction between groundwater (GM) and oceanic dynamics (OM). In this research,
15 we constructed a three-dimensional hydrodynamic model based on TELEMAC-3D (Hervouet, 2007) to simulate coastal OM.
16 Simultaneously, a GM using MODFLOW6(Hughes et al., 2017) was developed. To facilitate the coupling of these models, we
17 have employed the Telapy library(Audouin et al., 2017), a Python package designed to interface with Telemac, and Flopy(Bakker
18 et al., 2016), a set of Python modules that provide a powerful means of pre- and post-processing MODFLOW models. These
19 tools have been instrumental in enabling a loosely coupled approach, where the two models exchange information and
20 synchronize their simulations in an iterative process.

21 To validated the constructed model, different laboratory experiment published in the scientific literature studies has been
22 simulated confirm the accuracy and reliability of the coupled ocean and groundwater model. By validating the coupled model at
23 the laboratory scale and further building on the coupled model under tidal conditions, we aim to ensure its robustness and
24 applicability for broader, real-world scenarios, thus contributing to the advancement of coastal aquifer research and management.



1 **2 Coupling of numerical groundwater-ocean models**

2 **2.1. Groundwater Model**

3 **2.1.1. MODFLOW 6**

4 MODFLOW 6 is an object-oriented program that facilitates the integration of multiple models within a single simulation
5 framework (Hughes et al., 2017). This sixth core version by the USGS supports independent operation and information
6 exchange between models, enabling various interactions. The program is based on the principle of integrated finite differences
7 to calculate hydraulic head within a central grid, which is essential for simulating complex groundwater flow scenarios,
8 including saltwater intrusion.

9 In the context of groundwater flow, Darcy's Law is fundamental in describing fluid movement. For conditions of variable
10 density, the hydraulic head (∇h) form of Darcy's Law is expressed as:

$$11 \quad q = -K_0 \left(\nabla h + \frac{\rho - \rho_0}{\rho_0} g \nabla z \right) \quad (1)$$

12 Here, q represents the specific discharge vector, K_0 is the hydraulic conductivity, ρ is the local fluid density, ρ_0 is the
13 reference density, g is the acceleration due to gravity, and ∇z is the gradient of elevation.

14 MODFLOW 6 allows for the simulation of groundwater flow that accounts for variations in water density without the need to
15 convert between freshwater head and hydraulic head. Correction term is added directly to the calculations based on constant-
16 density flow to reflect the effects of density changes (Langevin et al., 2020a). This enhancement simplifies the simulation
17 process and improves the flexibility and accuracy in handling complex groundwater flow issues.

18 **2.1.2 Description of MODFLOW API**

19 The MODFLOW API (Hughes et al., 2022) has been instrumental in refining the boundary conditions and salinity values within
20 our groundwater model. By leveraging the API's BMI capabilities, we efficiently adjusted the General Head Boundary (GHB)
21 package to simulate dynamic coastal interactions without altering the source code. This flexibility allowed for precise control
22 over boundary head specifications, essential for capturing tidal influences and sea-level adjustments.

23 Moreover, the seamless integration with the Flopy library (Bakker et al., 2016) facilitated the coupling of the groundwater
24 model with an ocean model. Through this integration, the models exchanged critical data, such as salinity gradients and head
25 levels, enabling a holistic simulation of the groundwater-ocean system. This coupling was pivotal in understanding the complex
26 interplay between groundwater and ocean dynamics, particularly in the context of saltwater intrusion.

27 The combined use of MODFLOW API and Flopy streamlined the modeling process, providing a robust framework for
28 analyzing and managing coastal aquifer systems under varying salinity conditions.

29 **2.2. Ocean Model**

30 **2.2.1. Description of TELEMAC-3D Model**

31 The TELEMAC-3D model, part of the TELEMAC software suite (Hervouet, 2007), is a sophisticated Computational Fluid
32 Dynamics (CFD) tool designed for simulating diverse aquatic environments. The model accurately captures free-surface
33 dynamics through the solution of the non-hydrostatic Navier-Stokes equations, which are expressed as:



1
$$\rho \left(\frac{\partial \mathbf{v}}{\partial t} + \mathbf{v} \cdot \nabla \mathbf{v} \right) = -\nabla p + \nabla \tau + f_b \quad (2)$$

2 In this equation, ρ is density of the fluid, \mathbf{v} is velocity field, t is time, p is pressure, τ is stress tensor (Ocean diffusion), and
3 f_b is external forces (Coriolis and gravity).

4 To incorporate temperature and salinity into the TELEMAC-3D model, the fluid density ρ is modified as:

5
$$\rho = \rho_0 (1 - \alpha_T (T - T_0) + \beta_S (S - S_0)) \quad (3)$$

6 Where α_T is the thermal expansion coefficient, β_S is the haline contraction coefficient, T is temperature and S is salinity.

7 The buoyancy force f_b in the Navier-Stokes equation, which governs the fluid dynamics, is adjusted to include temperature
8 and salinity effects:

9
$$f_b = \rho_0 g (\alpha_T (T - T_0) - \beta_S (S - S_0)) \quad (4)$$

10 Model configuration is streamlined through the use of keywords in the ".cas" control file, which defines topography, boundary
11 conditions, and other essential parameters. The choice of time step is critical for the model's temporal resolution and overall
12 simulation accuracy, ensuring a faithful representation of the coupled groundwater-ocean system.

13 2.2.2. Description of Telapy

14 Telapy is a Python wrapper for the TELEMAC API that offers precise control over simulations (Audouin et al., 2017). It
15 enables users to pause simulations, access specific variables, and modify their values using a Fortran structure called
16 "instantiation." By adjusting TELEMAC's main subroutines, Telapy allows for step-by-step execution of hydraulic cases.
17 Python's versatility, portability, and extensive libraries make it an ideal tool for driving TELEMAC-MASCARET SYSTEM
18 APIs, enhancing simulation control and efficiency.

19 The development of Telapy addresses the complexity and accessibility challenges users faced with the Fortran API. With
20 Telapy, users can leverage Python's flexibility and expandability to simplify the simulation setup and execution process. The
21 rich library support in Python, such as NumPy and SciPy, facilitates complex data processing and analysis, making it a
22 powerful and intuitive tool for researchers and engineers in hydrological modeling and marine engineering.

23 2.3. Coupling Modflow and Telemac

24 2.3.1. Method Overview

25 In our research, we propose a bidirectional dynamic coupling method that can achieve a close integration of the ocean model
26 and the groundwater model. Specifically, with the help of the respective Python interfaces of Telemac and MODFLOW
27 (Telapy based on Telemac, Flopy based on MODFLOW), we have designed a coordination system that allows the two models
28 to alternate step-by-step during the simulation process and share necessary boundary condition information in real-time. This
29 includes parameters such as hydraulic head, temperature and salinity. Although the current implementation does not include the
30 simulation of solute pollutants, the coupling framework is designed to support the inclusion of these variables in future studies.
31 This coupling method aims to enhance the accuracy and reliability of simulation results by accurately reflecting the interaction
32 of the ocean-groundwater system.



1 In simulations of groundwater and seawater interaction, the traditional Henry problem assumes a constant salinity at the coastal
 2 boundary (Langevin et al., 2020b). However, we opted to refine this setup by designing the coastal boundary as a combination
 3 of a discharge area and a region maintaining seawater salinity. Yang introduced an adaptive salt mass flux boundary, which
 4 adjusts salinity based on the flow direction (Yang et al., 2013b). Consequently, at each time step, the boundary salinity is
 5 determined by the flow direction at the groundwater model's boundary conditions. For example, if water at a boundary point is
 6 flowing from the groundwater into the ocean, the salinity at that point is derived from the groundwater model. Conversely, if
 7 water is flowing from the ocean into the groundwater, the salinity would be based on the seawater model.

8 Our approach includes different key steps (fig 1):

9 1) At the start of computation, the model first obtains the state of the marine and groundwater models at their interface, including
 10 variables such as water level, salinity, and temperature.

11 2). Using the Telpy and Flopy interfaces, the temperature and salinity information of the marine model is transferred to the
 12 corresponding points of the groundwater model, and the information of the groundwater model is transferred to the corresponding
 13 points of the marine model. Data synchronization was achieved by directly transferring data between grid points that were
 14 spatially coincident in both model domains.

15 3). A single time step calculation is performed for the marine and groundwater models. Throughout the process, we pay special
 16 attention to the exchanged variables, including water level, salinity and temperature, to ensure they serve as inputs for the next
 17 time step of the model.

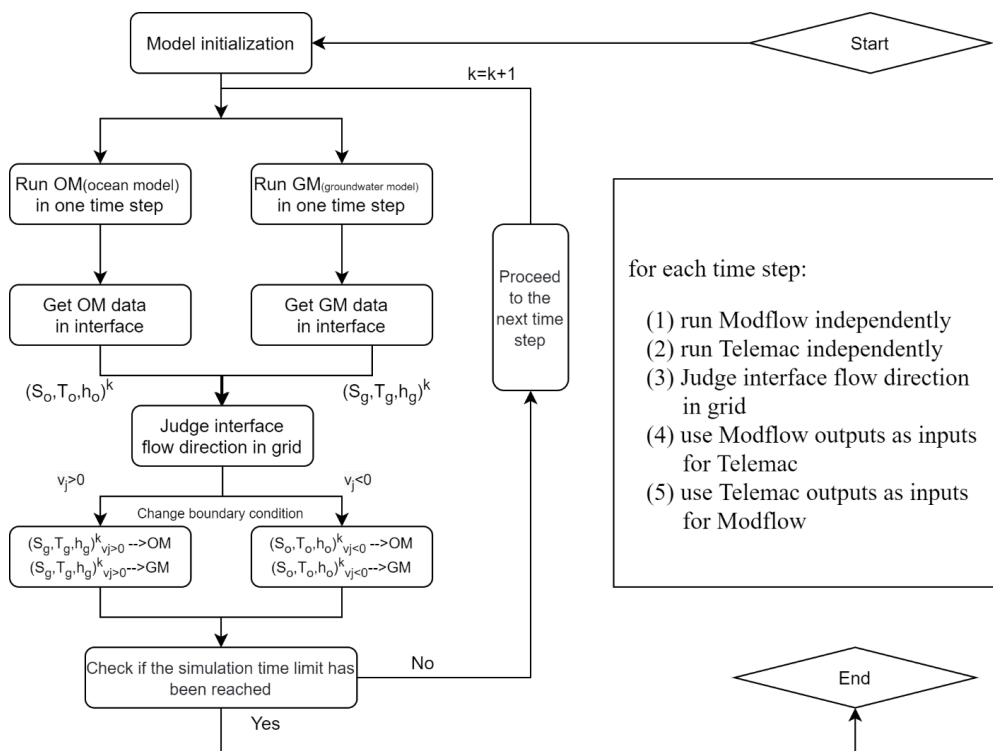


Fig. 1 Flowchart and Pseudo-code Illustrating the Process of Coupled Models



1 **2.3.2 Synchronized Time-Step Coupling**

2 A time-step coupling scheme was employed in this study to model the interaction between marine dynamics and groundwater
3 systems through the combined action of the Telemac and MODFLOW models(Yuan et al., 2011). In the coupling tidal case, the
4 Telemac model operated at a high frequency with a time step of 10 seconds, essential for capturing the rapid fluctuations of tides,
5 particularly critical for accurately reproducing the hydrodynamics features in regions where tidal energy is concentrated. Data,
6 including key hydrodynamic variables such as water levels and flow velocities, were outputted by the Telemac model every 600
7 seconds (every 10 minutes), serving as inputs to update the dynamic boundary conditions of the coastal region in the MODFLOW
8 model. Despite traditionally favoring longer time steps, the update frequency of the MODFLOW model was specifically tuned
9 within our coupling framework to match the output frequency of the Telemac model, ensuring that the groundwater model could
10 respond in real-time to changes in marine dynamics, accurately reflecting the immediate effects of tides on groundwater resources.
11 Throughout the three-day simulation period, the coupled modeling process iterated continuously: the Telemac model
12 independently ran with a 10-second time step to simulate oceanic processes, transferring its latest dataset to the MODFLOW
13 model every 600 seconds, which then promptly updated its coastal boundary conditions and continued simulating groundwater
14 flow, maintaining dynamic coordination and real-time information exchange between the two models. Time steps were carefully
15 calibrated, and data exchange frequency and processing algorithms were optimized, achieving a balance between high
16 synchronization among models while effectively managing the computational cost of the overall simulation, thereby harmonizing
17 simulation accuracy with computational efficiency.

18 **2.3.3 Integration of Salinity-Driven Hydrostatic Pressure**

19 In our research, the accurate setting of water head conditions at the land-sea interface has become a focal point, which is
20 critical for the precision of coupled ocean and groundwater models. Given that ocean salinity directly influences seawater
21 density(Fofonoff & Millard Jr, 1983), which in turn affects hydrostatic pressure, we have developed a comprehensive method to
22 obtain vertical salinity profiles at key coastal boundary locations. By obtaining detailed measurements of salinity at various
23 depths, we can calculate the density of seawater at each level, leading to precise estimations of corresponding hydrostatic
24 pressures. This measure is particularly crucial for simulating hydrological processes in coastal areas as it ensures that the boundary
25 conditions received by the groundwater model accurately reflect real-world hydrostatic pressures, rather than simply water depth.

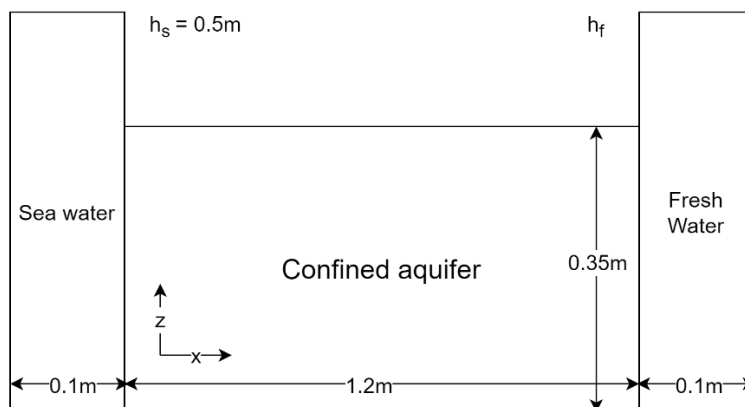
26 The benefits of adopting this method include enhanced simulation accuracy of groundwater models in coastal regions,
27 allowing them to more realistically depict the interactions between groundwater and the sea, which is essential for understanding
28 coastal hydrological processes. This approach improves the model's resilience to complex changes in marine environments,
29 especially in estuarine zones where salinity gradients are pronounced (Dias et al., 2021), capturing finer details of hydrodynamic
30 characteristics. Through the provision of more accurate pressure conditions, the accuracy of the model has been improved.



1 3 Model construction, validation and application

2 3.1. Validation of the coupled ocean-groundwater model.

3 3.1.1. Laboratory Groundwater model construction



4 **Fig. 2 Initial and boundary conditions of the numerical model**

5 Figure 2 illustrates the schematic diagram of the coupled numerical model, where the ocean component is depicted on the left,
6 the confined aquifer is in the middle, and the freshwater head is shown on the right. The model is used to study the effect of
7 changes in the freshwater head on seawater intrusion. A simplified hypothetical three-dimensional model was constructed based
8 on the confined aquifer at the center. The aquifer model extends 1.2 meters in length and is 0.35 meters thick, discretized into
9 approximately 4000 rectangular elements. The model employs no flow and no transport boundary conditions at the top and
10 bottom, while the freshwater boundary (right boundary) is set as a constant head boundary. The coastal boundary (left boundary)
11 is configured as a general head boundary, utilizing the CHD (Constant Head) and GHB (General Head Boundary)
12 subroutines (Bakker et al., 2016) for defining constant and mixed boundaries, respectively. This setup, common in saltwater
13 intrusion models (Voss & Souza, 1987), allows for the formation of a freshwater outflow zone above the saltwater recirculation
14 region. Comprehensive details on the model parameters can be found in the work of (Na et al., 2019). The model runs for a total
15 of 600 minutes, with a time interval consistent at 10 seconds.

16 3.1.2. Laboratory Ocean model construction

17 In the early stage of the research, based on the case of studying the impact of seawater density changes on SWI in the
18 laboratory (Na et al., 2019), we constructed a coupling model of ocean and groundwater.

19 For this study, the ocean model is configured adjacent to the groundwater model, with the ocean's surface set at 0.5m and
20 the bottom at 0m, establishing a constant head boundary condition. The model domain incorporates constant head boundaries
21 with specified salinity and temperature inputs on the left side, reflecting the influence of marine inflows.

22 Based on the ocean component depicted on the left side of Fig 2, we constructed a simplified three-dimensional ocean model.
23 The ocean model has a length of 0.1 meters and a depth of 0.5 meters, which is discretized into approximately 2,500 triangular
24 elements. The top of the model represents a free sea surface, and since the model is set to have a constant sea level, the left and
25 right sides are assigned constant heads, while the upper and lower boundaries are set as fixed interfaces. The model runs for a
26 total of 600 minutes, with a time interval consistent with the groundwater model at 10 seconds.

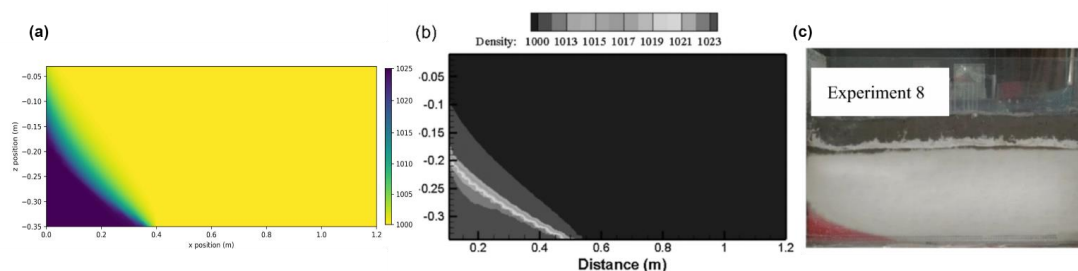
27 3.1.3. Result of laboratory coupled ocean-groundwater model.



1 We chose published laboratory experiments on seawater intrusion as the basis for validation (Na et al., 2019), given that the
 2 validation cases for the coupled model did not provide information on the marine component. Therefore, we focused on the
 3 groundwater model component during the validation process. These experiments meticulously recorded key parameters during
 4 the seawater intrusion process, such as salinity distribution and water level changes. We ran the coupled model using the same
 5 initial and boundary conditions as those specified in the selected case studies and compared our model output with the
 6 experimental data to assess the accuracy and reliability of the coupled model.

7 We compared the laboratory results figures, the numerical simulation figures published in the article, and the groundwater
 8 results from the coupled model. The validation was conducted by rigorously comparing the seawater toe location, the seawater
 9 height, and the time it takes for the model to reach a steady state.

10 Figure 3 shows that the coupled model successfully simulated the transient evolution of the saltwater wedge over time in a
 11 600-minute simulation when the water head height at the land boundary was 0.52 meters. The simulation results are relatively
 12 consistent with the laboratory observation data. This practical operation not only verifies the technical feasibility of the new
 13 coupled model, but also indicates that it can accurately reflect the actual situation.



14

15 **Fig.3 (a) Coupling model results in Groundwater part (b) Numerical model result in (Na et al., 2019) (c) Laboratory**
 16 **simulation results**

17 In this study, the CellBudgetFile module in Flopy was utilized to process the flux and flow direction of boundary units in
 18 the groundwater model at each time point during the entire simulation process. A comparison of the simulated data for Submarine
 19 Groundwater Discharge (SGD) and Recirculated Submarine Groundwater Discharge (RSGD) across different time periods in the
 20 two models reveals significant differences.

21 In terms of SGD simulation, the coupled model calculates an SGD value of $3.6 \times 10^{-2} \text{ m}^3$, slightly higher than the $3.4 \times 10^{-2} \text{ m}^3$
 22 calculated by the single model (see Table 1). This suggests that the coupled model more accurately reflects the complex material
 23 exchange between seawater and groundwater, thereby avoiding potential underestimation. For RSGD, the coupled model yields
 24 a value of $7.5 \times 10^{-3} \text{ m}^3$, which is up to 17% higher than the $6.4 \times 10^{-3} \text{ m}^3$ obtained from the single model. This difference highlights the
 25 coupled model's superior analytical capability and higher precision in capturing the saltwater recirculation mechanism.

26 **Table 1. Differences between the coupled model and the single groundwater model in simulating SGD.**

Unit: $\text{e}^{-2} \text{m}^3$	SGD	FSGD	RSGD
coupling model	3.6	2.8	0.8
single model	3.4	2.8	0.6

27 Traditional single models dealing with seawater intrusion (SWI) typically impose a constant salinity boundary condition,
 28 assuming that the salinity at the seawater-groundwater interface remains unchanged. This simplification overlooks the fact that
 29 freshwater discharge from the aquifer in real-world environments can reduce salinity at the sea-land interface, potentially leading
 30 to an underestimation of the effective discharge volume of SGD.

31 In contrast, the coupled model employs dynamic boundary conditions, which overcome this limitation. Within the
 32 framework of the coupled model, the boundary is no longer a static salinity barrier but becomes a responsive interface that adjusts
 33 with time and environmental conditions. When freshwater is discharged into the ocean through the SGD process, the dynamic
 34 boundary can immediately reflect the decrease in seawater salinity. Conversely, during the RSGD process, seawater back-



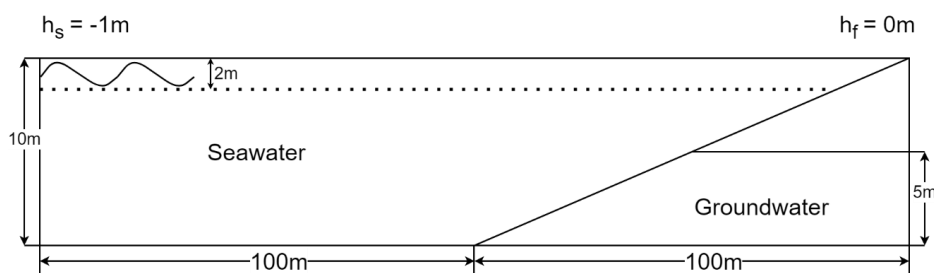
1 infiltration can increase groundwater salinity, and these changes are accurately captured by the model. This approach allows the
 2 model to not only simulate salinity distribution more accurately but also to reflect the natural fluctuations in water-salt exchange
 3 in coastal waters, thereby improving the realism of the simulation and the accuracy of SGD and RSGD quantification.

4 At the same time, the bidirectional feedback mechanism implemented in the coupled model further enhances this advantage.
 5 It ensures that the interaction between the ocean and the groundwater flow system is not unidirectional, but an interactive process.
 6 For example, changes in ocean tides not only affect the position and salinity of the seawater boundary, but also regulate the flow
 7 pattern of groundwater; and the rise and fall of groundwater levels can also feedback affect the hydrodynamic status of the
 8 nearshore marine area.

9 Although the improvement of the coupled model is not prominent in the basic case, when we introduce the coupled model
 10 into dynamic tides, due to its use of dynamic boundaries and bidirectional feedback mechanisms, the coupled model can help to
 11 understand those complex hydrogeochemical processes that are difficult for independent models to reveal.

12 3.2. Ocean-groundwater model with Tidal Boundary.

13 3.2.1. Ocean-groundwater model construction



14 **Fig. 4 Initial and boundary conditions of the tide numerical model**

15 Figure 4 presents a coupled numerical model schematic under tidal boundary conditions, with a sloping ocean on the left
 16 side and a confined aquifer on the right side. This coupled model aims to investigate the dynamics of submarine groundwater
 17 discharge and seawater intrusion under tidal influences.

18 The groundwater model component is a simplified three-dimensional structure with dimensions of 100 meters (length) × 50
 19 meters (width) × 5 meters (thickness), discretized into approximately 4000 rectangular elements. No-flow boundary conditions
 20 are applied at the top and bottom of the model. The freshwater boundary (right boundary) is set as a constant-head boundary at 0
 21 meters with a water temperature of 10 degrees Celsius. The coastal boundary (left side) is set as a general head boundary,
 22 defined using the Constant Head (CHD) and General Head Boundary (GHB) subroutines. The basic parameters used in the current
 23 simulation are shown in Table 2.

24 **Table 2. Parameters used in the numerical simulations of the groundwater part**

Parameter	Value
Aquifer porosity	0.35
Hydraulic conductivity	5e-3m/s
Saltwater density	1025 kg/m ³
Saltwater elevation	-1m
Freshwater density	1000 kg/m ³
Freshwater elevation	0m
The coefficient of molecular diffusion	1e-9m ² /s

25 The ocean model component utilizes the TELEMAC system, with dimensions of 200 meters (length) × 50 meters (width) ×
 26 10 meters (depth), and is discretized into approximately 2700 triangular elements. The top of the model represents the free surface
 27 of the sea, where tidal variations are introduced with a range from -2 meters to 0 meters. The seabed is set at -10 meters. The left
 28 boundary of the domain is specified with tidal boundary conditions representing the tidal water level, with salinity set to a constant



1 35 ppt, and temperature varying sinusoidally from 20 to 25 degrees Celsius with each tidal state to reflect the influence of marine
2 inflow. The right boundary serves as a fixed boundary, simulating the actual coastline.

3 The model operation is divided into two phases: the first phase simulates until the system reaches a steady state; the second
4 phase lasts for 72 hours, with a time step of 10 minutes, and the groundwater model and the ocean model had the same time step.

5 **3.2.2. Result of ocean-groundwater model**

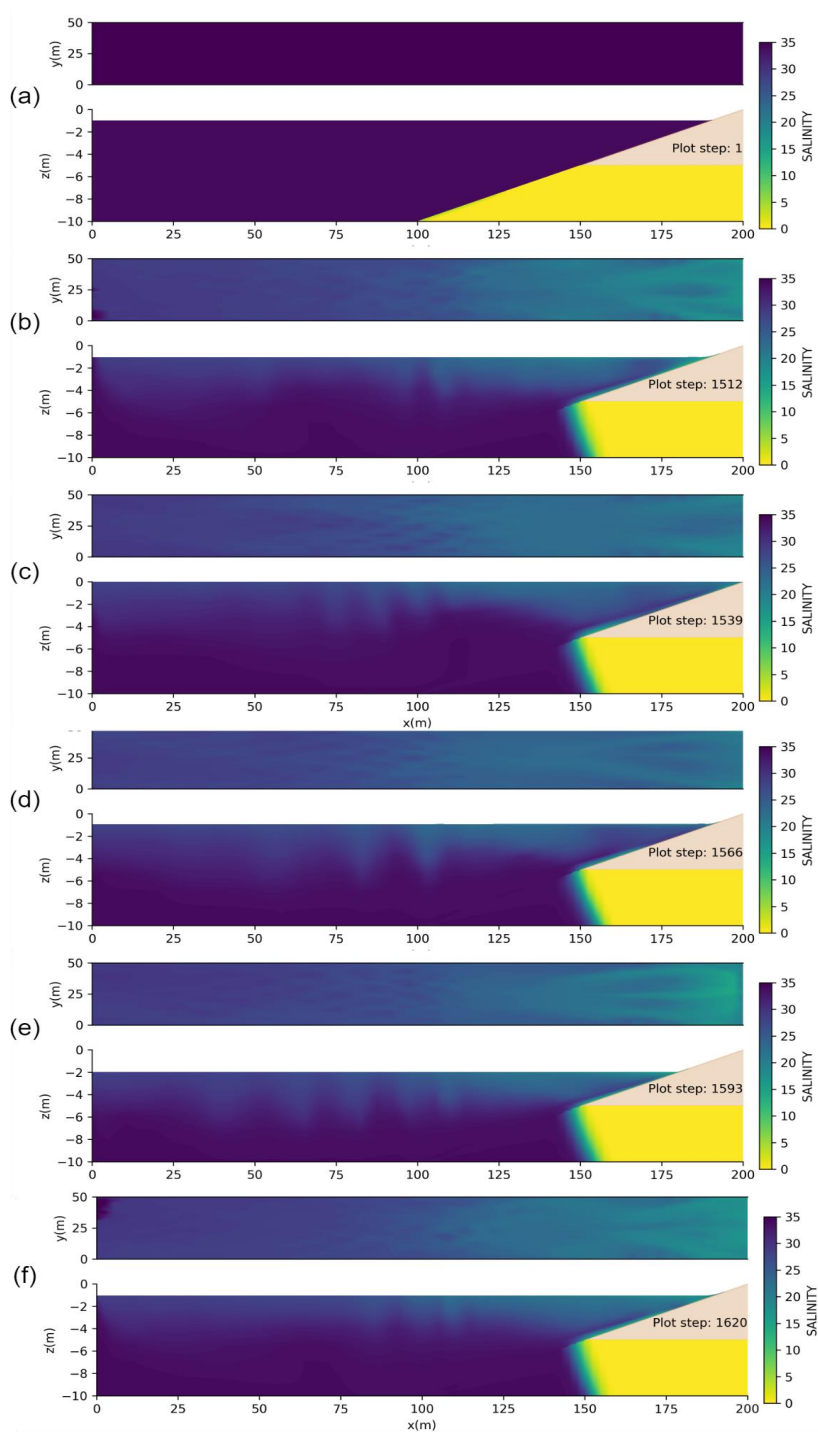
6 This study investigates the dynamic interactions between ocean and groundwater systems, particularly focusing on the
7 salinity distribution and its evolution over time as depicted in Fig. 5. The upper part of the figure shows a top-down view of the
8 ocean model, while the lower part presents a side view of the coupled model.

9 Initially, the model starts with a distinct salinity gradient, where the ocean side is characterized by a uniformly high
10 salinity of 35 (purple), while the adjacent land aquifer is under a pressurized freshwater condition (yellow). This setup creates a
11 sharp boundary between saltwater and freshwater, setting the stage for subsequent interactions.

12 As the system evolves towards equilibrium (Fig. 5b), a stable salinity distribution emerges, characterized by the formation
13 of a saltwater wedge that extends from the ocean into the aquifer. This wedge structure is indicative of the balance achieved
14 between the ocean's saline water and the freshwater outflow driven by Submarine Groundwater Discharge (SGD). The
15 boundary between the saltwater and freshwater becomes more defined, showing a delicate balance where freshwater from the
16 aquifer spreads over the ocean surface and gradually mixes with seawater.

17 A complete sinusoidal tidal cycle (b-f) is shown to illustrate the effects of tidal fluctuations on this balance. The impacts of
18 these fluctuations are clearly visible during high tide (Fig. 5c) and low tide (Fig. 5e). During high tide (b-c), the rising sea level
19 drives more saline water into the aquifer, causing the saltwater wedge to expand further inland, as indicated by the increased
20 red area. Conversely, at low tide, the retreating sea level allows some saltwater to flow back into the ocean, reducing the
21 wedge's inland penetration and allowing the freshwater in the aquifer to recover. This cyclical process highlights the significant
22 impact of tidal forces on the salinity dynamics at the sea-land interface.

23 Additionally, the lag effect of tidal fluctuations on seawater intrusion is clearly demonstrated. During high tide (Fig. 5c), the
24 rising sea level causes the saltwater wedge to rapidly advance inland. However, it can be observed that even though the sea level
25 has started to rise, the maximum extent of the saltwater wedge does not immediately reach its peak but takes some time to fully
26 intrude. Conversely, during low tide (Fig. 5e), when the sea level drops, the saltwater wedge begins to retreat. However, the
27 saltwater does not immediately exit the aquifer; instead, it shows a slow withdrawal trend. Even after the sea level has dropped,
28 the saltwater remains within the aquifer for some time. This phenomenon indicates that despite the rapid changes in tidal levels,
29 the process of seawater intrusion exhibits a certain degree of lag. This reflects that the response speed of the groundwater system
30 is slower than the changes in sea level.

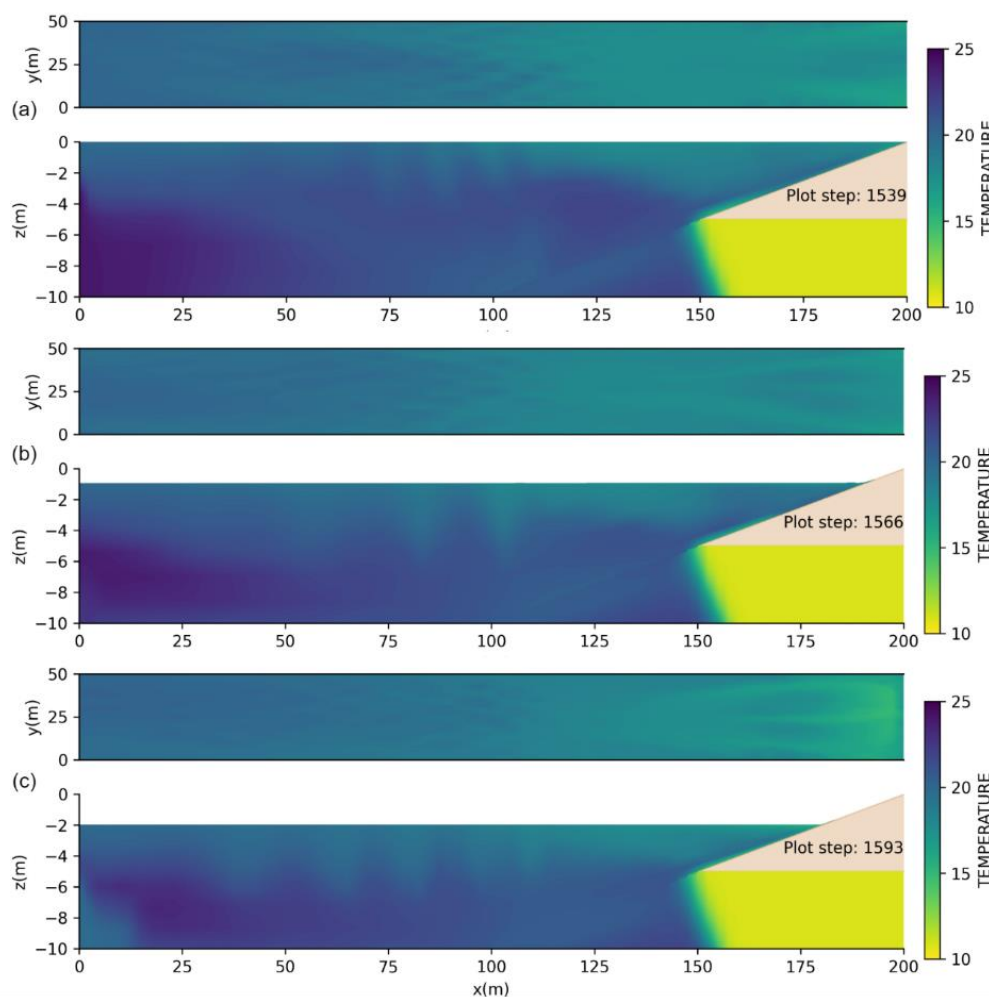


1

2

3

Fig. 5 Coupling model simulation of salinity patterns throughout tidal cycles depicted in top and vertical views
(a)Initial moment **(b)**Tidal Start **(c)** High Tide **(d)** First Tidal Stand **(e)** Low Tide **(f)** Second Tidal Stand



1

2 **Fig. 6 Temperature patterns throughout tidal cycles depicted in top and vertical views (a) High Tide moment (b) Tidal**
3 **Stand moment (c) Low Tide moment**

4 Similar to salinity distribution, temperature variations are also influenced by the dynamics of groundwater discharge
5 (SGD). Specifically, temperature changes in the upper layer of the ocean are observed due to SGD. Fig 6 illustrates three
6 distinct time points, reflecting the impact of submarine groundwater discharge on ocean temperatures as the tide transitions
7 from high to low.

8 Figure 6a depicts the scenario when the tide is at its highest point. At this stage, cooler water from the aquifer spreads
9 along the land-sea interface to the ocean surface, creating a distinct cold front that is particularly evident in the upper layers of
10 the sea. With the tide at its peak, there is maximum seawater coverage, and a large volume of warmer seawater enters from the
11 left side, resulting in a concentrated temperature distribution with a noticeable temperature gradient.

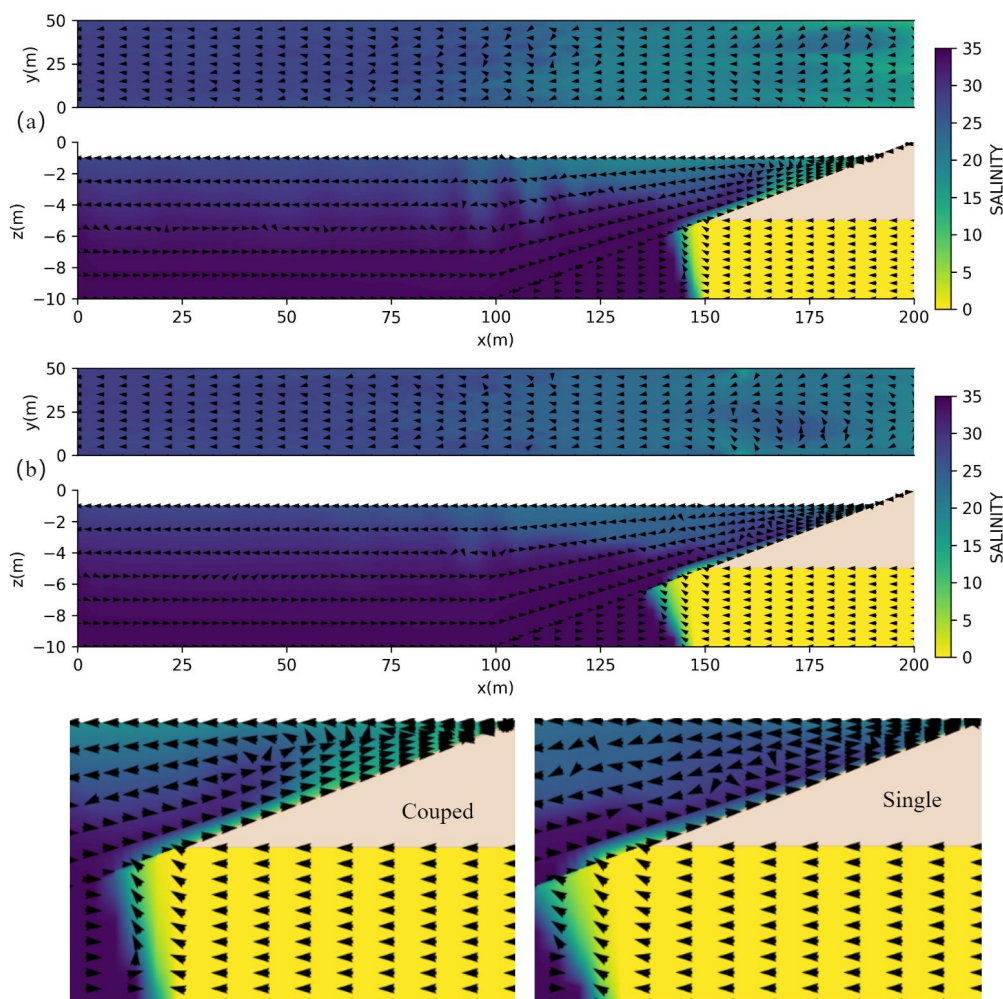
12 As the tide begins to recede but has not yet reached its lowest point (Fig. 6b), the colder groundwater discharged is
13 gradually extending outward due to the decreasing tide, mixing with the surrounding warmer seawater. This leads to a more
14 uniform temperature distribution and a reduction in the temperature gradient.



1 Figure 6c describes the situation when the tide reaches its lowest point. At this time, the seawater covers the smallest area,
2 allowing the colder groundwater discharged to accumulate more easily on the ocean surface, awaiting the next tidal cycle for
3 further mixing.

4 3.2.3. Comparison of the ocean-groundwater model with single model

5 To comprehensively assess the advantages of the coupled model, this study also separately ran the standalone ocean model
6 and groundwater model. In the ocean model, a specified flux boundary condition was set at the top of the interface between the
7 ocean and the confined aquifer to simulate submarine groundwater discharge. In the groundwater model, a general head boundary
8 (GHB) condition with a fixed salinity of 35 was applied at the land-sea interface to simulate interactions between seawater and
9 groundwater. By comparing the simulation results of the standalone models and the coupled model (Fig. 7), it becomes clearer
10 that the coupled model can more effectively capture the dynamic changes in complex environments.



11

12 Fig. 7 Comparison of salinity and velocity between two models from top and vertical views (a) Coupled Model (b)
13 Single Model



1 In the ocean top-view of Fig 7, dynamic variations caused by the interaction between the ocean surface and groundwater are
2 captured in the coupled model. The arrows on the ocean surface in the coupled model, which indicate flow direction and velocity,
3 appear somewhat disordered. This is due to the complex local flows generated by groundwater discharge in the coupled model.
4 Unlike a conventional ocean model, the coupled model integrates dynamic submarine groundwater discharge (SGD), which
5 induces localized convection, eddies, and small-scale mixing effects near the seafloor. This phenomenon indicates that the
6 coupled model more accurately represents the complex conditions found in real-world environments.

7 The observed patterns in the figure suggest that regions with disordered arrows extend towards the ocean due to groundwater
8 discharge. In the coupled model, the discharge area is confined to the upper portion of the land-sea interface, where complex
9 interactions between upwelling groundwater and seawater create multiple turbulence zones. Within these areas, flow exhibits
10 irregular and rapidly fluctuating patterns. The extension of disordered arrow regions toward the ocean implies that groundwater
11 discharge not only introduces a new mechanism for material transport into the ocean but also provides additional kinetic energy,
12 thereby enhancing mixing processes in nearshore waters.

13 In the view on the right side of Fig 7, it is evident that more freshwater accumulates at the ocean surface in the coupled
14 model compared to the standalone model. This is due to the faster discharge rate and higher volume of groundwater discharge in
15 the coupled model.

16 In the cross-sectional view of groundwater, Fig 7a shows the shape of seawater intrusion in the coupled model, while Fig
17 7b presents the shape in the single groundwater model, which is comparatively more gradual than that of the coupled model.
18 Using the CellBudgetFile module, we obtained groundwater flow velocities at the submarine discharge outlet for both models.
19 Results show that the discharge velocity in the coupled model is 30% higher than in the single model.

20 In the single model, the land-sea boundary salinity is fixed at a relatively high level, resulting in higher pressure heads at
21 the boundary. This reduces the head difference with inland areas and slows groundwater flow velocity. This slower groundwater
22 discharge effectively resists seawater intrusion, resulting in a more gradual saline wedge shape with a shallower intrusion depth.
23 In contrast, the coupled model incorporates a gradation of boundary salinity from the surface to the bottom, with lower salinity
24 levels in the upper zones and lower pressure heads. This leads to faster groundwater flow. The increased discharge rate decreases
25 freshwater pressure and creates a head difference that encourages seawater to advance inland to fill the gap created by fresh water
26 discharge. This pressure differential accelerates seawater intrusion into the aquifer, resulting in a steeper saline wedge and deeper
27 intrusion depth.

28 Comparing the shapes of seawater intrusion between the single and coupled models demonstrates that boundary conditions
29 and discharge rates significantly impact seawater intrusion patterns. The coupled model provides a more accurate representation
30 of the actual hydrodynamic conditions at the land-sea interface, offering a more precise perspective for understanding seawater
31 intrusion mechanisms.

32 **3.2.4. The Impact of Tides on SGD**

33 The influence of tides on submarine groundwater discharge (SGD) is significant, characterized by pronounced periodic
34 variations (Li et al., 2016). Specifically, during high tide, the increased seawater pressure not only suppresses SGD but may even
35 cause seawater to flow back into the aquifer, exacerbating seawater intrusion. Conversely, during low tide, as seawater pressure
36 decreases, the discharge of groundwater into the ocean significantly increases, indicating that SGD exhibits non-steady-state
37 characteristics (Fang et al., 2021b).

38 In the comparison between the coupled model and the single model, we distinguish the types of submarine groundwater
39 discharge based on salinity. Due to the mixing of freshwater and brackish water at the land-sea interface, we simplify the
40 classification by considering water with salinity less than 5 as freshwater. Our findings show that during a 24-hour steady-state
41 observation and a 72-hour tidal fluctuation period, as illustrated in Table 3, the SGD for the coupled model is 97.5 m³, representing
42 a 17% increase compared to the single model's 83.1 m³. The total amount of freshwater groundwater discharge (FSGD) is
43 comparable between the two models. However, the recirculated submarine groundwater discharge (RSGD) in the coupled model
44 is 39.4 m³, a 54% increase over the single model's 25.6 m³. This indicates that RSGD contributes almost entirely to the increase



1 in SGD.

2 **Table 3. Analysis of Submarine Groundwater Discharge (SGD) in Coupled and Single Models.**

unit:m ³	Coupled model			Single model		
SGD	FSGD	RSGD	SGD	FSGD	RSGD	
97.50	58.10	39.40	83.10	57.50	25.60	

3 Tidal fluctuations can significantly alter the ratio of RSGD to FSGD. As shown in Table 4, under tidal influence, the
 4 performances of SGD in coupled models and single models exhibit significant dynamic variations, with the coupled model
 5 providing a more accurate reflection of the tidal-induced groundwater flow characteristics. Under steady-state conditions, the
 6 SGD values for the coupled model and single model are $25.50 \times 10^{-5} \text{ m}^3/\text{s}$ and $22.90 \times 10^{-5} \text{ m}^3/\text{s}$, respectively. In the coupled
 7 model, FSGD and RSGD are $16.80 \times 10^{-5} \text{ m}^3/\text{s}$ and $8.70 \times 10^{-5} \text{ m}^3/\text{s}$, while in the single model, they are $16.70 \times 10^{-5} \text{ m}^3/\text{s}$ and
 8 $6.20 \times 10^{-5} \text{ m}^3/\text{s}$, respectively. These results indicate that under steady-state conditions, the coupled model captures more
 9 recirculated water flow, demonstrating a closer exchange with oceanic water.

10 **Table 4. Dynamic Variations of submarine groundwater discharge (SGD) Under Tidal Influence between Coupled**
 11 **model and Single model.**

unit: $10^{-5} \text{ m}^3/\text{s}$	Coupled model			Single model		
	SGD	FSGD	RSGD	SGD	FSGD	RSGD
Steady state	25.50	16.80	8.70	22.90	16.70	6.20
High tide	16.70	12.20	4.50	5.20	5.10	0.10
Middle tide	28.00	17.40	10.60	26.10	18.20	7.90
Low tide	46.20	21.30	24.90	46.40	28.10	18.30

12 Under the influence of tidal fluctuations, SGD, FSGD, and RSGD in both coupled and single models exhibit periodic
 13 changes. At high tide, due to the increase in seawater pressure, the SGD for the coupled model and the single model decrease to
 14 $16.70 \times 10^{-5} \text{ m}^3/\text{s}$ and $5.20 \times 10^{-5} \text{ m}^3/\text{s}$, respectively. During this period, RSGD significantly declines, with values of 4.50×10^{-5}
 15 m^3/s in the coupled model and only $0.10 \times 10^{-5} \text{ m}^3/\text{s}$ in the single model. This phenomenon suggests that seawater pressure
 16 suppresses groundwater discharge at high tide, reducing the flow of recirculated water and allowing freshwater discharge to
 17 dominate.

18 As tidal levels decline, SGD gradually increases, reaching its maximum value at low tide, where the SGD in the coupled
 19 model and single model rises to $46.20 \times 10^{-5} \text{ m}^3/\text{s}$ and $46.40 \times 10^{-5} \text{ m}^3/\text{s}$, respectively. During low tide, RSGD and FSGD in the
 20 coupled model peak at $24.90 \times 10^{-5} \text{ m}^3/\text{s}$ and $21.30 \times 10^{-5} \text{ m}^3/\text{s}$, respectively, with RSGD slightly exceeding FSGD. This indicates
 21 that the decrease in tidal levels facilitates greater recirculation of seawater into the aquifer, enhancing the discharge of recirculated
 22 water.

23 Overall, tidal effects significantly influence the total amount of SGD and the ratio of FSGD to RSGD, particularly evident
 24 during high and low tide. The coupled model, by incorporating the dynamic processes of oceanic and groundwater interactions,
 25 can more accurately reflect the changes in groundwater discharge driven by tidal forces, including the suppression effects during
 26 high tide and the enhancement effects during low tide. Compared to the single model, the coupled model is more representative
 27 of the real ocean-groundwater interactions, exhibiting more complex discharge dynamics, thereby contributing to a deeper
 28 understanding of the mechanisms behind tidal-driven submarine groundwater discharge.



1 4 Conclusion

2 This study innovatively addresses the long-standing challenge of independently modeling groundwater and ocean systems
3 by implementing a coupled framework that effectively exchanges data at the land-sea interface. This research led us to formulate
4 the following pivotal conclusions:

5 1. This study has developed a coupled model for simulating the interaction between groundwater and ocean systems. The
6 model's potential and accuracy have been preliminarily validated through experimental case studies, demonstrating its
7 effectiveness in this complex environmental context. The coupled model successfully simulated the transient evolution of the
8 saltwater wedge over time, showing relative consistency with laboratory observation data, thereby verifying the technical
9 feasibility and accuracy of the model in reflecting actual conditions.

10 2. The coupled model developed in this study demonstrates significant advantages in simulating the interaction between
11 groundwater and ocean systems, particularly in dealing with dynamic boundary conditions and mixing zones in coastal areas.
12 Compared with traditional single groundwater models, the coupled model not only captures fluctuations in salinity and
13 temperature but also specifically considers the effects of mixing zones that are often overlooked. This integrated simulation
14 approach allows for more precise definition of boundary conditions and realistically reflects the hydrogeological and geochemical
15 processes at the interface, thereby enhancing the accuracy and comprehensiveness of the simulation. The coupled model's
16 dynamic boundary conditions and bidirectional feedback mechanisms provide a more accurate reflection of the complex material
17 exchange between seawater and groundwater, avoiding potential underestimation of effective discharge volumes.

18 3. The coupled model employed in this study vividly illustrates the dispersion of Submarine Groundwater Discharge (SGD)
19 in the marine environment, offering a novel perspective on the interactions at the groundwater-ocean interface. Tidal fluctuations
20 were found to significantly influence the rate and pattern of SGD, thereby modulating the input of nutrients and potential
21 contaminants into the ocean, and revealed the intricate mechanisms of their diffusion, transformation, and accumulation within
22 marine ecosystems. Moreover, the dynamic response of the ocean has a substantial impact on the pathways and spatial distribution
23 of SGD, underscoring the necessity of incorporating an oceanographic viewpoint in studies related to SGD. The coupled model's
24 ability to simulate the effects of tidal influences on SGD and seawater intrusion provides a more accurate understanding of these
25 complex hydrogeochemical processes.

26 To build upon the findings of this study and further advance our understanding of the complex interactions between
27 groundwater and ocean systems, the following research directions are proposed:

28 1). Explore how variations in bathymetry and tidal patterns, as well as different hydraulic conductivities, affect the dynamics
29 of seawater intrusion (SWI) and submarine groundwater discharge (SGD). Additionally, investigate the impact of temperature
30 and salinity changes on the movement and dispersion of SGD in coastal environments.

31 2). Integrate biogeochemical processes into the coupled model to simulate the chemical transformations that occur as SGD
32 interacts with the ocean. Develop reactive transport models that consider the reactions between groundwater constituents and the
33 marine environment.

34 3). Apply the coupled model to real-world coastal systems to validate the model against observed data. Deploy additional
35 observational points in both terrestrial and marine environments to collect critical data for model calibration and validation.
36 Conduct scenario analysis to predict the impacts of climate change, such as rising sea levels and increased storm events, on SGD
37 and SWI.



1 **Code/Data availability**

2 Some or all data, models, or code generated or used during the study are available from the corresponding author by request.

3 **Author contribution**

4 Jiangyue Jin (First Author): Conceptualization, Methodology, Code, Writing - Original Draft;

5 Manuel Espino: Theoretical guidance for the ocean model; Supervision, editing & revising the manuscript;

6 Daniel Fernández: Theoretical guidance for the groundwater model; editing & revising the manuscript

7 Albert Folch (Corresponding Author): Theoretical guidance for the groundwater model, Funding Acquisition, Resources,

8 Supervision, Review & Editing.

9 **Competing interests**

10 The authors declare that they have no conflict of interest.



1 References

- 2 Arévalo-Martínez, D. L., Haroon, A., Bange, H. W., Erkul, E., Jegen, M., Moosdorf, N., Schneider von Deimling, J., Berndt, C.,
3 Böttcher, M. E., Hoffmann, J., Liebetrau, V., Mallast, U., Massmann, G., Micallef, A., Michael, H. A., Paasche, H.,
4 Rabbel, W., Santos, I., Scholten, J., ... Weymer, B. A. (2023). Ideas and perspectives: Land–ocean connectivity through
5 groundwater. *Biogeosciences*, 20(3), 647–662. <https://doi.org/10.5194/bg-20-647-2023>
- 6 Audouin, Y., Goeury, C., Zaoui, F., Ata, R., Essebtey, S. E. I., Torossian, A., & Rouge, D. (2017). *Interoperability applications of*
7 *TELEMAC-MASCARET System*.
- 8 Bakker, M., Post, V., Langevin, C. D., Hughes, J. D., White, J. T., Starn, J. J., & Fienen, M. N. (2016). Scripting MODFLOW
9 Model Development Using Python and FloPy. *Groundwater*, 54(5), 733–739. <https://doi.org/10.1111/gwat.12413>
- 10 Cao, T., Han, D., & Song, X. (2021). Past, present, and future of global seawater intrusion research: A bibliometric analysis.
11 *JOURNAL OF HYDROLOGY*, 603, 126844. <https://doi.org/10.1016/j.jhydrol.2021.126844>
- 12 Carabin, G., & Dassargues, A. (1999). Modeling groundwater with ocean and river interaction. *WATER RESOURCES*
13 *RESEARCH*, 35(8), 2347–2358. <https://doi.org/10.1029/1999WR900127>
- 14 Dassargues, A., Brouyere, S., Carabin, G., & Schmitz, F. (1996). Conceptual and computational challenges when coupling a
15 groundwater model with ocean and river models. In A. A. Aldama, J. Aparicio, C. A. Brebbia, W. G. Gray, I. Herrera, &
16 G. F. Pinder (Eds.), *COMPUTATIONAL METHODS IN WATER RESOURCES XI, VOL 1: COMPUTATIONAL*
17 *METHODS IN SUBSURFACE FLOW AND TRANSPORT PROBLEMS* (pp. 77–84). Computational Mechanics
18 Publications Ltd. <https://www.webofscience.com/wos/woscc/full-record/WOS:A1996BG41G00009>
- 19 Dias, J. M., Pereira, F., Picado, A., Lopes, C. L., Pinheiro, J. P., Lopes, S. M., & Pinho, P. G. (2021). A Comprehensive Estuarine
20 Hydrodynamics-Salinity Study: Impact of Morphologic Changes on Ria de Aveiro (Atlantic Coast of Portugal). *Journal*
21 *of Marine Science and Engineering*, 9(2), Article 2. <https://doi.org/10.3390/jmse9020234>
- 22 Dong, Y., Zhang, X., & Yi, L. (2024). Hypoxia exerts greater impacts on shallow groundwater nitrogen cycling than seawater
23 mixture in coastal zone. *Environmental Science and Pollution Research*, 31(31), 43812–43821.
24 <https://doi.org/10.1007/s11356-024-34045-8>
- 25 Fang, Y., Zheng, T., Zheng, X., Yang, H., Wang, H., & Walther, M. (2021a). Influence of Tide-Induced Unstable Flow on Seawater
26 Intrusion and Submarine Groundwater Discharge. *WATER RESOURCES RESEARCH*, 57(4), e2020WR029038.
27 <https://doi.org/10.1029/2020WR029038>
- 28 Fang, Y., Zheng, T., Zheng, X., Yang, H., Wang, H., & Walther, M. (2021b). Influence of Tide-Induced Unstable Flow on Seawater
29 Intrusion and Submarine Groundwater Discharge. *Water Resources Research*, 57(4), e2020WR029038.
30 <https://doi.org/10.1029/2020WR029038>
- 31 Fofonoff, N. P., & Millard Jr, R. C. (1983). *Algorithms for the computation of fundamental properties of seawater*.
32 <https://doi.org/10.25607/OBP-1450>
- 33 Haque, A., Salama, A., Lo, K., & Wu, P. (2021). Surface and Groundwater Interactions: A Review of Coupling Strategies in
34 Detailed Domain Models. *Hydrology*, 8(1), Article 1. <https://doi.org/10.3390/hydrology8010035>
- 35 Hervouet, J.-M. (2007). *Hydrodynamics of free surface flows: Modelling with the finite element method*. Wiley.
- 36 Hughes, J. D., Langevin, C. D., & Banta, E. R. (2017). Documentation for the MODFLOW 6 framework. In *Documentation for*
37 *the MODFLOW 6 framework* (USGS Numbered Series 6-A57; Techniques and Methods, Vols. 6-A57). U.S. Geological
38 Survey. <https://doi.org/10.3133/tm6A57>
- 39 Hughes, J. D., Russcher, M. J., Langevin, C. D., Morway, E. D., & McDonald, R. R. (2022). The MODFLOW Application
40 Programming Interface for simulation control and software interoperability. *Environmental Modelling & Software*, 148,
41 105257. <https://doi.org/10.1016/j.envsoft.2021.105257>
- 42 Kim, J., Cho, H.-M., & Kim, G. (2015). 228Ra flux in the northwestern Pacific marginal seas: Implications for disproportionately
43 large submarine groundwater discharge. *Ocean Science Journal*, 50(2), 195–202. [https://doi.org/10.1007/s12601-015-](https://doi.org/10.1007/s12601-015-0015-3)
44 0015-3
- 45 Langevin, C. D., Panday, S., & Provost, A. M. (2020a). Hydraulic-Head Formulation for Density-Dependent Flow and Transport.



- 1 *Groundwater*, 58(3), 349–362. <https://doi.org/10.1111/gwat.12967>
- 2 Langevin, C. D., Panday, S., & Provost, A. M. (2020b). Hydraulic-Head Formulation for Density-Dependent Flow and Transport.
- 3 *Groundwater*, 58(3), 349–362. <https://doi.org/10.1111/gwat.12967>
- 4 Lewandowski, J., Meinikmann, K., & Krause, S. (2020). Groundwater–Surface Water Interactions: Recent Advances and
- 5 Interdisciplinary Challenges. *Water*, 12(1), Article 1. <https://doi.org/10.3390/w12010296>
- 6 Li, X., Hu, B. X., & Tong, J. (2016). Numerical study on tide-driven submarine groundwater discharge and seawater recirculation
- 7 in heterogeneous aquifers. *Stochastic Environmental Research and Risk Assessment*, 30(6), 1741–1755.
- 8 <https://doi.org/10.1007/s00477-015-1200-8>
- 9 Lin, Z., Zhang, G., Zou, H., & Gong, W. (2024). Salt intrusion dynamics in a well-mixed sub-estuary connected to a partially to
- 10 well-mixed main estuary. *Ocean Science*, 20(1), 181–199. <https://doi.org/10.5194/os-20-181-2024>
- 11 Liu, Y., Jiang, Y., Zhang, S., Wang, D., & Chen, H. (2023). Application of a Linked Hydrodynamic–Groundwater Model for
- 12 Accurate Groundwater Simulation in Floodplain Areas: A Case Study of Irtys River, China. *Water*, 15(17), 3059.
- 13 Martínez-Pérez, L., Luquot, L., Carrera, J., Marazuela, M. A., Goyetche, T., Pool, M., Palacios, A., Bellmunt, F., Ledo, J., Ferrer,
- 14 N., del Val, L., Pezard, P. A., García-Orellana, J., Diego-Feliu, M., Rodellas, V., Saaltink, M. W., Vázquez-Suñé, E., &
- 15 Folch, A. (2022). A multidisciplinary approach to characterizing coastal alluvial aquifers to improve understanding of
- 16 seawater intrusion and submarine groundwater discharge. *Journal of Hydrology*, 607, 127510.
- 17 <https://doi.org/10.1016/j.jhydrol.2022.127510>
- 18 Michael, H. A., Mulligan, A. E., & Harvey, C. F. (2005). Seasonal oscillations in water exchange between aquifers and the coastal
- 19 ocean. *Nature*, 436(7054), 1145–1148. <https://doi.org/10.1038/nature03935>
- 20 Moore, W. S., & Joye, S. B. (2021). Saltwater Intrusion and Submarine Groundwater Discharge: Acceleration of Biogeochemical
- 21 Reactions in Changing Coastal Aquifers. *Frontiers in Earth Science*, 9. <https://doi.org/10.3389/feart.2021.600710>
- 22 Na, J., Chi, B., Zhang, Y., Li, J., & Jiang, X. (2019). Study on the influence of seawater density variation on sea water intrusion
- 23 in confined coastal aquifers. *Environmental Earth Sciences*, 78(24), 669. <https://doi.org/10.1007/s12665-019-8684-3>
- 24 Nguyen, T. T. M., Yu, X., Pu, L., Xin, P., Zhang, C., Barry, D. A., & Li, L. (2020). Effects of Temperature on Tidally Influenced
- 25 Coastal Unconfined Aquifers. *WATER RESOURCES RESEARCH*, 56(4). <https://doi.org/10.1029/2019WR026660>
- 26 Perumal, M., Sekar, S., & Carvalho, P. C. S. (2024). Global Investigations of Seawater Intrusion (SWI) in Coastal Groundwaters
- 27 in the Last Two Decades (2000–2020): A Bibliometric Analysis. *Sustainability*, 16(3), Article 3.
- 28 <https://doi.org/10.3390/su16031266>
- 29 Ramatlapeng, G. J., Atekwana, E. A., Ali, H. N., Njiloh, I. K., & Ndong, G. R. N. (2021). Assessing salinization of coastal
- 30 groundwater by tidal action: The tropical Wouri Estuary, Douala, Cameroon. *JOURNAL OF HYDROLOGY-REGIONAL*
- 31 *STUDIES*, 36, 100842. <https://doi.org/10.1016/j.ejrh.2021.100842>
- 32 Ramesh, R., Chen, Z., Cummins, V., Day, J., D’Elia, C., Dennison, B., Forbes, D. L., Glaeser, B., Glaser, M., Glavovic, B.,
- 33 Kremer, H., Lange, M., Larsen, J. N., Le Tissier, M., Newton, A., Pelling, M., Purvaja, R., & Wolanski, E. (2015). Land–
- 34 Ocean Interactions in the Coastal Zone: Past, present & future. *Anthropocene*, 12, 85–98.
- 35 <https://doi.org/10.1016/j.ancene.2016.01.005>
- 36 Santos, I. R., Chen, X., Lecher, A. L., Sawyer, A. H., Moosdorf, N., Rodellas, V., Tamborski, J., Cho, H.-M., Dimova, N.,
- 37 Sugimoto, R., Bonaglia, S., Li, H., Hajati, M.-C., & Li, L. (2021). Submarine groundwater discharge impacts on coastal
- 38 nutrient biogeochemistry. *NATURE REVIEWS EARTH & ENVIRONMENT*, 2(5), 307–323.
- 39 <https://doi.org/10.1038/s43017-021-00152-0>
- 40 Slomp, C. P., & Van Cappellen, P. (2004). Nutrient inputs to the coastal ocean through submarine groundwater discharge: Controls
- 41 and potential impact. *Journal of Hydrology*, 295(1–4), 64–86. <https://doi.org/10.1016/j.jhydrol.2004.02.018>
- 42 Turner, R. K., Subak, S., & Adger, W. N. (1996). Pressures, trends, and impacts in coastal zones: Interactions between
- 43 socioeconomic and natural systems. *Environmental Management*, 20(2), 159–173. <https://doi.org/10.1007/BF01204001>
- 44 Voss, C. I., & Souza, W. R. (1987). Variable density flow and solute transport simulation of regional aquifers containing a narrow
- 45 freshwater-saltwater transition zone. *Water Resources Research*, 23(10), 1851–1866.
- 46 <https://doi.org/10.1029/WR023i010p01851>



- 1 Wang, X., Geng, X., Sadat-Noori, M., & Zhang, Y. (2022). Editorial: Groundwater-Seawater Exchange and Environmental
- 2 Impacts. *Frontiers in Water*, 4. <https://doi.org/10.3389/frwa.2022.928615>
- 3 Yang, J., Graf, T., Herold, M., & Ptak, T. (2013a). Modelling the effects of tides and storm surges on coastal aquifers using a
- 4 coupled surface-subsurface approach. *JOURNAL OF CONTAMINANT HYDROLOGY*, 149, 61–75.
- 5 <https://doi.org/10.1016/j.jconhyd.2013.03.002>
- 6 Yang, J., Graf, T., Herold, M., & Ptak, T. (2013b). Modelling the effects of tides and storm surges on coastal aquifers using a
- 7 coupled surface-subsurface approach. *Journal of Contaminant Hydrology*, 149, 61–75.
- 8 <https://doi.org/10.1016/j.jconhyd.2013.03.002>
- 9 Yu, X., Xin, P., & Lu, C. (2019). Seawater intrusion and retreat in tidally-affected unconfined aquifers: Laboratory experiments
- 10 and numerical simulations. *Advances in Water Resources*, 132, 103393.
- 11 <https://doi.org/10.1016/j.advwatres.2019.103393>
- 12 Yuan, L.-R., Xin, P., Kong, J., Li, L., & Lockington, D. (2011). A coupled model for simulating surface water and groundwater
- 13 interactions in coastal wetlands. *Hydrological Processes*, 25(23), 3533–3546. <https://doi.org/10.1002/hyp.8079>
- 14